Journal of Physics: Conference Series

PAPER • **OPEN ACCESS**

Particle-in-cell simulations of an inverted sheath

To cite this article: I Gomez *et al* 2020 *J. Phys.: Conf. Ser.* **1492** 012004

Particle-in-cell simulations of an inverted sheath

I Gomez[1,2], A Valič[1], T Gyergyek[3,2,4], S Costea[2] and J Kovačič[2,3]

[1]University of Ljubljana, Faculty of Mathematics and Physics, Jadranska 19, 1000 Ljubljana, Slovenia
[2]Jožef Stefan Institute, Jamova 39, 1000 Ljubljana, Slovenia
[3]University of Ljubljana, Faculty of Electrical Engineering, Tržaška 25, 1000 Ljubljana, Slovenia

E-mail: tomaz.gyergyek@fe.uni-lj.si

Abstract. An inverted sheath is simulated by particle-in-cell simulations using the XPDP1 code. It is shown that a stable monotonically decreasing potential structure can be formed in a bounded plasma system, where positive ions and source electrons are injected from the right-hand side (source) electrode and emitted electrons are injected from the left-hand side (collector) electrode. Such inverted sheath structure is created in the absence of collisions or ionization, provided that the ratio of injection fluxes of both electron groups is large enough. In this work preliminary results are reported and some effects of different ion injection are illustrated.

1. Introduction

Electron emission plays an important role in the physics of plasma-surface interactions and is a central element in many plasma related applications and phenomena. Because of its importance, the problem of potential formation in a plasma in front of an electron emitting electrode has been studied by many authors [1-6]. A widely accepted picture of the potential formation in front of electron emitting electrodes can be very briefly summarized as follows. If a floating electrode is immersed in a plasma, more electrons than positive ions will hit it on average because of the larger electron mobility. As a consequence, the electrode will bias negatively with respect to plasma. If the electrode starts emitting electrons, the floating potential starts to increase and becomes less negative with respect to plasma potential. As long as the electron emission is not too big, the potential profile remains monotonic and a negative electric field at the electrode accelerates the emitted electrons through the sheath into the plasma. At a certain point the so-called critical emission is achieved. At that point, the electric field in front of the electrode becomes equal to zero. If the electron emission is increased further, the electric field reverses its direction and starts accelerating the electrons back to the electrode. Such emission is called supercritical or space charge limited, because the emitted electrons start to accumulate in front of the electrode and form a negative space charge in front of it. As a consequence, a potential well is formed in front of the electrode and the potential becomes non-monotonic. Such a potential dip is often called a virtual cathode. If the emission increases further, the floating potential does not change much; only the excess of positive space charge increases and the potential well becomes deeper. This apparent "saturation" of the floating potential with respect to electron emission is used for plasma potential measurements with emissive probes [7].

[4] To whom any correspondence should be addressed.

For a long time it was believed that the floating potential of an emissive probe cannot exceed the plasma potential, although Marek et al. [8] reported about such an observation in 2008. Only a few years later, Campanell argued that at a very high electron emission the floating potential of the electrode could become positive with respect to the plasma potential [9-12]. He named such a potential structure an inverted sheath. In this work an inverted sheath is simulated by the XPDP1 code [13].

2. Simulations

The Berkeley XPDP1 code [13] is used to perform the simulations. A plasma system bounded by two planar electrodes is simulated. The length of the system is 2 mm and it is divided into 2000 cells so that the length of 1 cell is 1 micron. Electrons emitted from the left-hand-side electrode (collector, located at x = 0) (index 2) are injected with a half-Maxwellian velocity distribution. From the right hand side electrode (source, located at $x = L$ = 2 mm), singly charged positive ions (index i) and electrons (index 1) are injected also with a half-Maxwellian velocity distributions. The source electrode is always at zero (reference) potential, while the collector is electrically floating with respect to the source. The code XPDP1 requires input in SI units and gives output in the same units. Thus, the real electron mass and charge are used. For the ion mass, deuterium is selected with $m_i = 3.34358\times10^{-27}$ kg. The electrons from the source (source electrons) are injected with a flux j_1 = 100 A/m^2, while the electrons emitted from the collector are injected with a flux j_2 = 432500 A/m^2. In this work, results for three different ion injection fluxes j_i are presented. These fluxes are: j_i = 0.4, 0.5 and 0.6 A/m^2. The system is initially empty and the particle injection start from both electrodes simultaneously. When the number of superparticles becomes constant, steady state is reached and then the results are read. In all cases, the emitted electrons are injected with a thermal velocity v_{2xth} = 229685 m/s, which correspond to a temperature kT_{2x} = 0.3 eV. Here k is the Boltzmann constant and $v_{2thx} = \sqrt{kT_{2x} / m_e}$, where m_e is the electron mass. The thermal velocity of the ions is v_{ithx} = 6922 m/s, which corresponds to an ion temperature kT_{ix} = 1 eV; and the thermal velocity of the source electrons is v_{1thx} = 1326087 m/s, which corresponds to a source electron temperature kT_{1x} = 10 eV.

3. Results

The presentation of the results starts with the potential and electric field profiles, which are shown in figure 1. In the top of the figure the axial profiles of the potential $\Phi(x)$ are shown for three different ion injections j_i = 0.4, 0.5 and 0.6 A/m^2. A larger ion injection results in a slightly larger potential in the middle of the system. The potential decreases monotonically from the collector towards the source. Quite strong potential drops can be observed in front of the collector and in front of the source. In the central part of the system, the potential profile is much flatter. This indicates that the source sheath and the collector sheath are formed in front of the source and in front of the collector. This is confirmed by the electric field profiles $E_x(x)$. In front of the collector, the electric field is really large, but then it drops very quickly by several orders of magnitude reaching a minimum in the middle of the system, and then increasing again close to the source. This can be seen much better when the electric field is shown in a logarithmic scale. If the ion injection is increased, the electric field at the source also increases. The electric field plots in a logarithmic scale show clearly that in the middle of the system the electric field reaches a minimum, which is quite close to zero.

Figure 2 presents the particle and space charge density profiles. The particle densities $n(x)$ are shown for all three ion injections in a logarithmic scale. The density of the emitted electrons at the collector drops very steeply by several orders of magnitude, then the profile becomes flat, and then there is again a drop in front of the source. The density profiles of the ions and source electrons decrease slowly from the source towards the collector; only very close to the collector is the ion density drop more pronounced. The space charge density profile is shown in the bottom of figure 2. A large negative space charge caused by the emitted electrons can be observed in front of the collector. The inset shows the profile on an expanded scale. There it can be seen that in the middle of the system neutrality is reached and close to the source there is a small surplus of positive space charge due to the ions. The locations of the minimum of the electric field (figure 1) and of the zero space charge density (figure 2) coincide very well.

In figure 3, phase space plots of all three particle species are shown, together with the temperature profiles. Results are shown only for the smallest ion injection, j_i = 0.4 A/m^2. The top left figure presents the phase space for the source electrons. It can be seen very clearly how all the electrons are accelerated towards the collector by the electric field and there are no electrons with positive velocity v_x in the direction towards the source. In top right figure, the phase space for the emitted electrons is presented. These electrons are

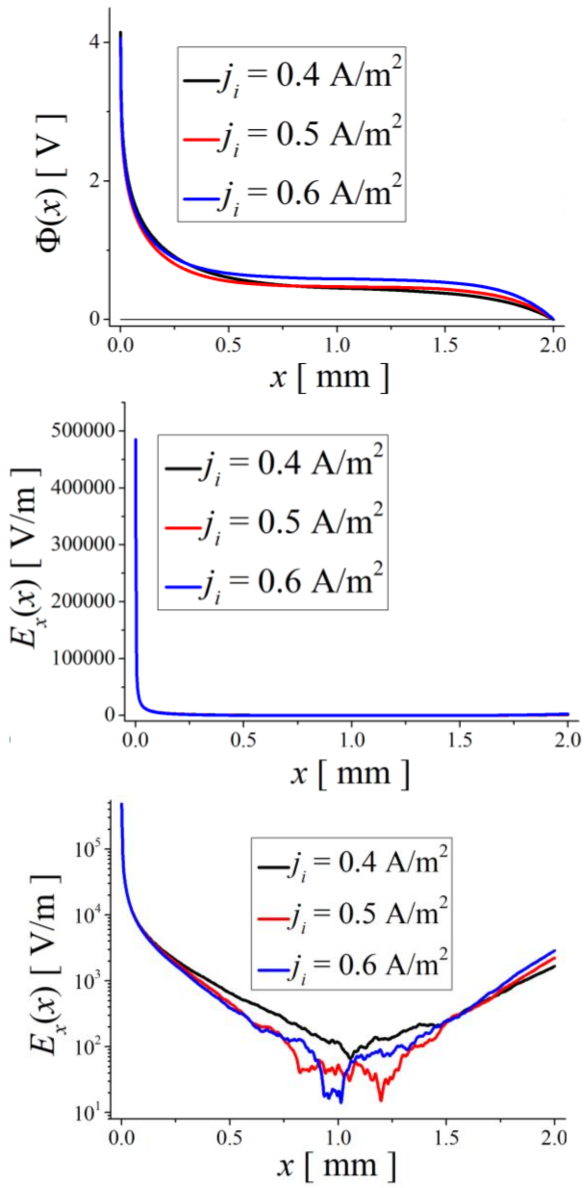

Figure 1. Axial profiles of the potential Φ(x) and the electric field $E_x(x)$ in linear and logarithmic scale for three different ion injections j_i.

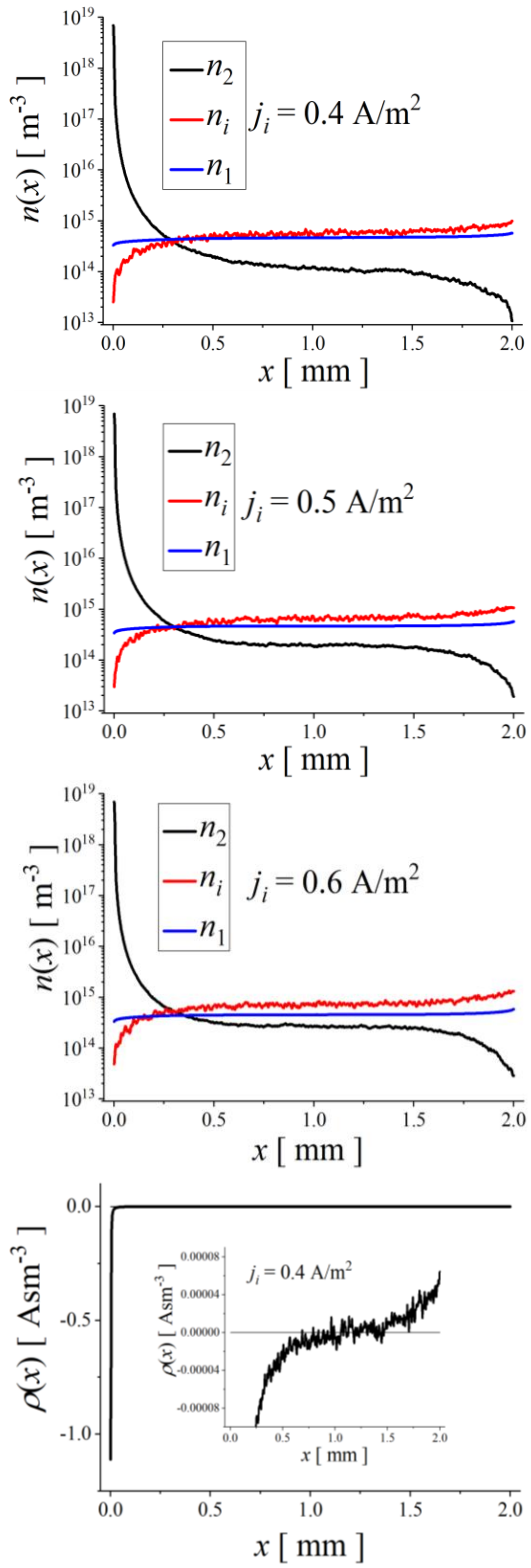

Figure 2. Particle density $n(x)$ profiles shown for three different ion injections. Space charge density profile shown only for the smallest ion injection. j_i = 0.4 A/m^2.

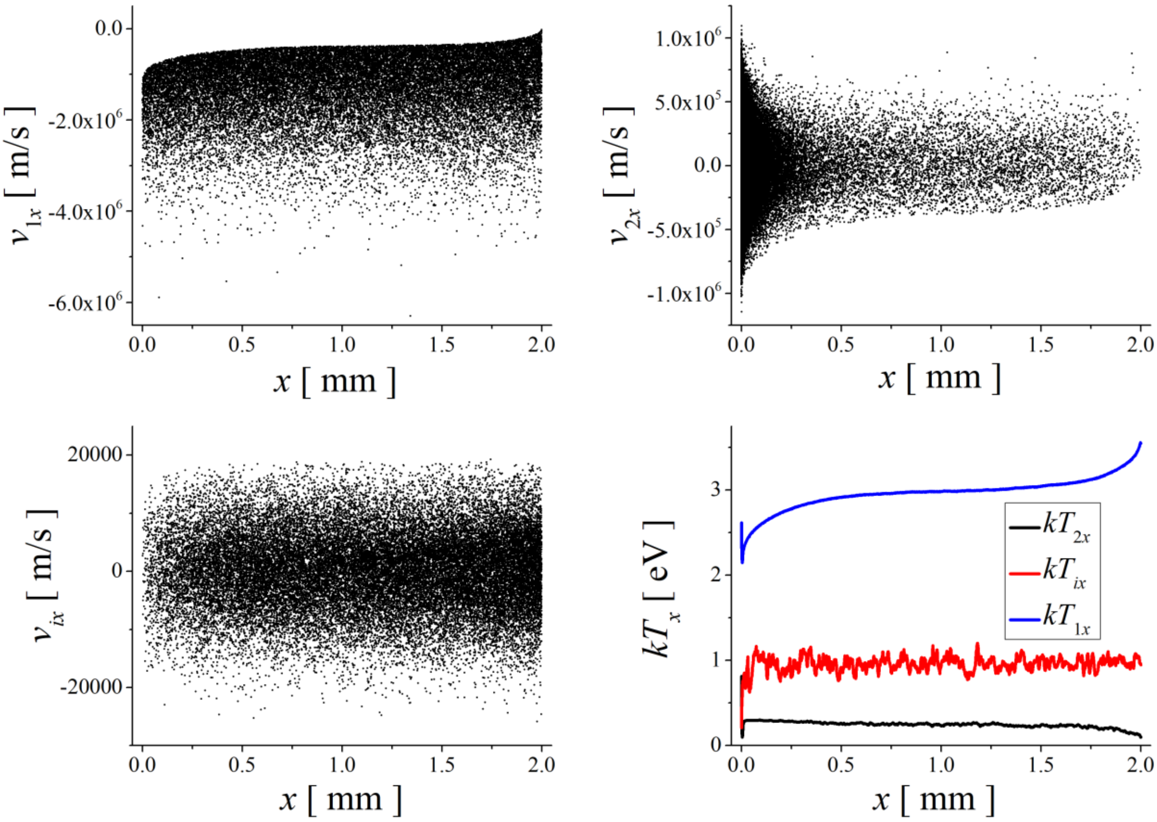

Figure 3. Phase space plots and temperature profiles for all three particle species. It is clearly seen that the velocity distributions of all three particle species have cut-offs. Ion injection is j_i = 0.4 A/m^2.

injected from the collector, but are repelled back towards it by the electric field. Only those that leave the collector with large enough velocity can reach the source, so a clear cut-off can be observed for the negative values of v_x. The bottom left figure shows the phase space for the ions. The ions are injected from the source towards the collector, but are accelerated back towards the source by the electric field. Only those that have sufficient energy when they leave the source can reach the collector; consequently, a clear cut-off can be seen for the positive values of v_x. In the bottom right graph, the axial profiles are shown of the temperatures kT_x for all three particle groups. The source electrons are injected with a thermal velocity corresponding to 10 eV. Because they are strongly accelerated, their distribution function becomes narrower, which results in their substantial cooling (around 3 eV, instead of 10 eV). The temperatures of the ions and emitted electrons, on the other hand, remain very close to the nominal temperature of their injection – 0.3 eV for the emitted electrons and 1 eV for the ions. This is caused by the repulsion of these species by the electric field, so that the distribution functions contain positive and negative velocities. The small cut-offs do not decrease the temperature substantilly.

4. Conclusions

One dimensional particle-in-cell simulations of an inverted sheath using the Berkeley XPDP1 [13] code are presented. These simulations confirm that a stable monotonically decreasing potential structure can be formed even in the absence of collisions or ionizations [10, 12]. In earlier simulations [14], we were not able to obtain stable potential profiles, most probably because the electron emission was too small. Note that in the present work the electric current density of the emitted electrons j_2 exceeds that of the injection source electrons j_1 by a factor of more than 4000. The results of these simulations can be modelled by a kinetic model based on cut-off Maxwellian velocity distribution functions of individual particle species. These distribution functions are obtained on the basis of the assumption that the potential is either monotonically increasing (collector negative with respect to the source) or decreasing (collector positive with respect to the source). For increasing potentials, such models are well developed, while for the decreasing potentials they are still in the initial stage [17].

Acknowledgements
This work was partially supported by the grants P2-0405, P2-0073 and BI-FR/CEA/17-19-002 of the Slovenian Research Agency and EUROfusion grant ENR-MFE19.CEA-06. This work has been carried out within the framework of the EUROfusion Consortium and has received funding from the Euratom research and training program 2014-2018 and 2019-2020 under grant agreement No 633053. The views and opinions expressed herein do not necessarily reflect those of the European Commission.

References

[1] Hobbs G D and Wesson J A 1967 *Plasma Phys*. **9** 85-7
[2] Franklin R N and Han W E 1988 *Plasma Phys. Controlled Fusion* **30** 771-84
[3] Schwager L A 1993, *Phys. Fluids* B **5** 631-45
[4] Ordonez C A 1977 *Phys. Rev*. E **55** 1858-71
[5] Takamura S, Ohno N, Ye M Y and Kuwabara T 2004 *Contrib. Plasma Phys.* **44** 126-37
[6] Din A 2013 *Phys. Plasmas* **20** 093505
[7] Sheehan J P and Hershkowitz N 2011 *Plasma Sources Sci. Technol.* **20** 063001
[8] Marek A, Jilek M, Pickova I, Kudrna P, Tichy M, Schrittwieser R and Ionita C 2008 *Contrib. Plasma Phys*. **48** 491-6
[9] Campanell M D, Khrabrov A V and Kaganovich I D 2012 *Phys. Rev. Letters* **108** 255001
[10] Campanell M D 2013 *Phys. Rev.* E **88** 033103
[11] Campanell M D and Umansky M V 2016 *Phys. Rev. Letters* **116** 085003
[12] Campanell M D and Umansky M V 2017 *Phys. Plasmas* **24** 057101
[13] Verboncoeur J P, Alves M V, Vahedi V and Birdsall C K 1993 *J. Comp. Phys.* **104** 321-8
[14] Gyergyek T and Kovačič J 2013 *Contrib. Plasma Phys*. **53** 189-201
[15] Schwager L A and Birdsall C K 1990 *Phys. Fluids* B **2** 1057-68
[16] Gyergyek T, Jurčič-Zlobec B and Čerček M 2008 *Phys. Plasmas* **15** 063501
[17] Gomez I, Gyergyek T and Kovačič J 2019 *46th EPS Conf. Plasma Phys. 8-12 July 2019 Milan Italy* p4.3004 http://ocs.ciemat.es/EPS2019PAP/pdf/P4.3004.pdf